Field test measuring the effect of preloading on soil properties affecting the seismic response and numerical simulation

F. Lopez-Caballero & A. Modaresi-Farahmand-Razavi
Laboratoire MSS-Mat CNRS UMR 8579, Ecole Centrale Paris Grande Voie des Vignes, 92290 Châtenay-Malabry, France

C. Stamatopoulos & P. Peridis
Stamatopoulos and Associates, 5 Isavron street, Athens 11471, Greece

SUMMARY:
The results of an elaborate field preloading research study on a liquefaction-susceptible site are presented. Preloading was applied by a temporary embankment 9m high. Prior and after preloading, borings with standard penetration tests, cone penetration tests and geophysical studies were performed. During the process of embankment construction and demolition, settlements were recorded versus time at different locations. A finite element modelling is carried out in order to evaluate the effects of embankment construction and demolition in terms of settlements and structural behaviour. Soil improvement was simulated and compared with measurements. The measurements and the numerical models illustrated the decrease in liquefaction susceptibility induced by preloading. In addition, a numerical parametric analysis is performed so as to quantify the impact of the uncertainties associated with the input signal on both the ground motion and the apparition of liquefaction phenomena.

Keywords: preloading, soils, sands, liquefaction, field test, numerical analysis

1. INTRODUCTION

Saturated sandy layers that are horizontal, or have a small inclination to the horizontal, run the risk of earthquake-induced liquefaction. Design codes (e.g. European Standard, 2003) demand of the practicing engineer the estimation of the liquefaction risk. The factor of safety against liquefaction, estimated versus depth, is defined as the ratio of the *in-situ* cyclic soil strength by the cyclic stress ratio resulting from the design earthquake (European Standard, 2003). In cases where the factor of safety against liquefaction takes values close to, or less than, unity, soil improvement is an effective way to mitigate the liquefaction risk by increasing the cyclic soil strength (Committee of Earthquake Engineering et al, 1985). Preloading is a temporary loading applied at a construction site, to improve subsurface soils primarily by increasing density and horizontal stress (Stamatopoulos and Kotzias, 1985). The purpose of this work is to investigate the effect of preloading in the cyclic strength of different soils both in-situ and numerically.

2. FIELD TEST

A complete field test on a liquefaction-susceptible sandy site with data of (a) the SPT and CPT strength and Vs versus depth before and after preloading and (b) changes in the horizontal stress and void ratio of the soil as a result of preloading do not exist in the literature. Such a field test was performed on a liquefaction-susceptible site under a recent research project funded by the European Union. The Albanian partners of the project S. Allkja and L. Bozo of Altea Geostudio Co. proposed a liquefaction-susceptible site in Porto Romano, 10km North of Durress in the Albanian coast (Fig. 1). Four geotechnical borings were performed by Altea Geostudio Co. to verify the suitability of the site.

In the location of the preload test, four (4) soil borings with sampling and Standard Penetration Tests

performed in borings (SPT) every meter to 15m (total length of borings = 60m) were performed. Piezometers were installed in two borings to measure the elevation of the water table. A standard laboratory testing program including classification, compressibility and strength tests was also performed. In addition, three (3), Cone Penetration Tests (CPT) soundings to 15m (total hole lengths is 45m), and down-hole surveys for measuring the shear wave velocity Vs were performed. Fig. 3 gives the average CPT and Vs measurements versus depth. Table 1 gives the soil layers that exist in the site based on the geotechnical investigations and their compressibility estimated from oedometer tests. The water table depth was measured at 1.5m. Fig. 2a gives the initial and maximum past vertical effective stress versus depth, estimated from oedometer tests.

The most efficient (requiring less volume of fill for given surcharge) design of embankment is to use a truncated-cone-shaped preload earth fill. A 50m diameter fill, 9m high, 13m diameter at the crest was used. A ramp was also constructed in order to perform construction. Construction started on 6/6/2011. This date corresponds to day 0 in all the graphs given below. The soil used to construct the embankment was sandy. Compaction of the layer was performed with a vibrator. Field density tests were performed to verify compaction. During the placement of the preload embankment, an unexpected slide occurred due to excess rate of construction. Fortunately, the instruments were not damaged during the slide. In addition, this slide provided interesting data regarding the correct rate of construction in the construction of preloading embankments when a soft clay layer exists on shallow depths. After the slide, part of the embankment was demolished and reconstructed at a considerably slower rate. Construction terminated, after reaching an embankment height of 9m from initial ground level after settlement (that means 9.54m above unsettled ground level) on 10/8/2011, or day 60. The embankment stayed until 10/10/11, or 126 days after the start of construction, or 60 days after construction. Then, the rate of settlement was very small, less than 0.001m/day. The embankment was removed in 11 days. The following instruments were placed to measure settlements: (1) Horizontal Inclinometer in level ground, along a radius of the embankment-to-be-constructed, (2) Five settlement plates on ground level at different locations of the embankment base to measure the settlement by topographic means, particularly to verify the settlement measured by the other means, (3) A Magnetic extensiometer very near the centre of the base of the embankment-to-be-constructed to measure the ground displacement versus depth at 2m increments at depths 0 to 20m. In addition, horizontal pressure cells were placed at the locations given in Table 2. In each horizontal cell location, pore pressure transducers were also installed in order to measure the excess pore pressure, and from the horizontal stress and excess pore-pressure to extract the effective horizontal stress. Regarding settlement measurements, it was first observed that settlement measurements of all devices were consistent with each other. Fig. 4 gives the settlement versus time in terms of location measured by the inclinometer. The following can be observed: the magnitude of settlement is less than one meter and the time required for the settlement rate to decrease to values less than 0.001m/day is similar to previous preload applications (Stamatopoulos et al., 2005, Stamatopoulos and Kotzias, 1985). Due to disturbance as a result of instrument placement, the initial measurement of horizontal stress is not reliable. Thus, only the change of horizontal stress due to embankment construction and demolition can be analyzed. Fig. 5 gives the measured change in effective horizontal stress in terms of time and device. Some instrument numbers are missing, because these instruments failed.

After the removal of the embankment identical field investigations were performed in order to investigate the post-improvement soil strength. Fig. 3 gives the average CPT and Vs measurements versus depth after soil improvement.

Table 1. Soil layers that exist in the site based on the geotechnical investigations and virgin and reloading coefficient of compressibility

Depth	Layer description	classification symbol	Cc	Cr
0-3.5m	Silty Clay	MH,CH	0.52	0.02
3.5-7m	Medium Gravel with silty sand	SP-SM, GW-GM	0.05	0.01
7m-15m	Fine Sand and Silt	ML, SM, CL-ML	0.06	0.02

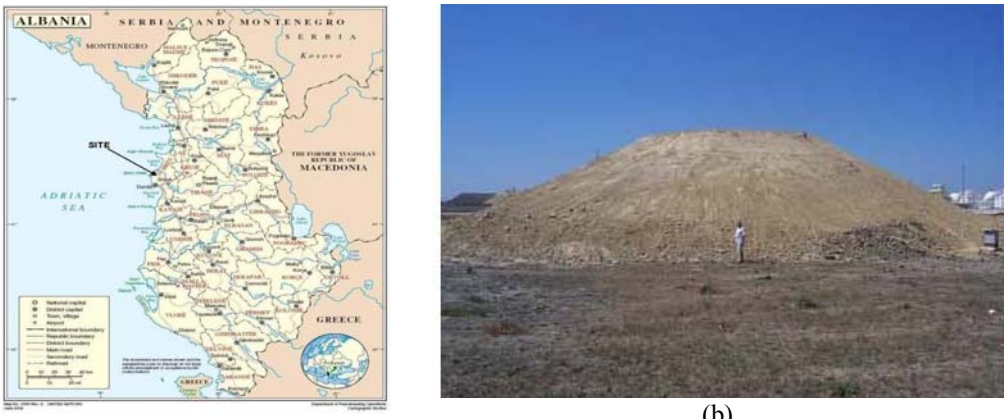

(a) (b)

Figure 1. (a) General location of the site, (b) Photography of the embankment at top height

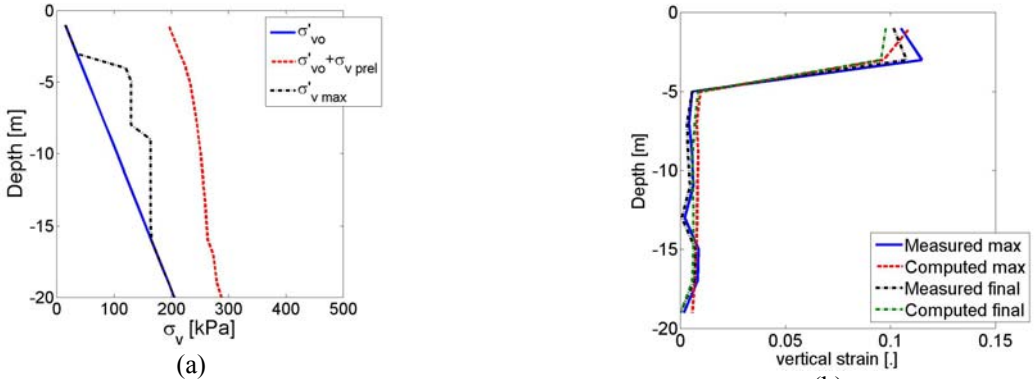

(a) (b)

Figure 2. Porto Romano. (a) Initial, maximum and maximum past vertical effective stress versus depth. (b). Maximum and final vertical strain versus depth measured using the magnetic extensiometer and predictions

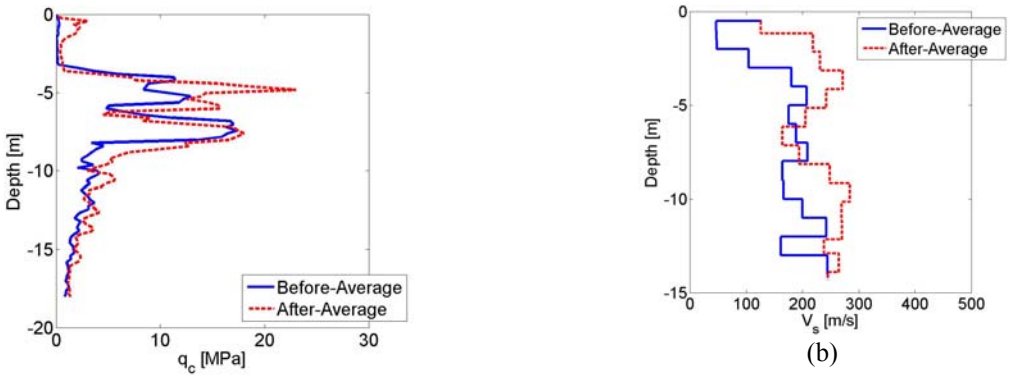

(a) (b)

Figure 3. Profiles of average CPT and Vs values before and after soil improvement

Table 2. The location of the horizontal pressure cells, and prediction of the residual horizontal stress

	Depth (m)	r (m)	Δσz (kPa)	σ'g (kPa)	OCRa	OCRb	Δσh-res (kPa)	Δσh-m (kPa)	Ratio
H3	11.62	16.50	65.16	197.54	1.33	1.00	15.01	14.00	0.93
H5	6.40	6.50	163.80	108.80	2.51	1.29	23.88	30.00	1.26
H6	5.85	16.50	77.40	99.45	1.78	1.41	7.19	8.60	1.20
H8	3.25	6.50	176.40	55.25	4.19	1.00	15.27	20.00	0.71
H9	2.50	16.50	140.40	42.50	4.30	1.00	8.04	25.00	1.13

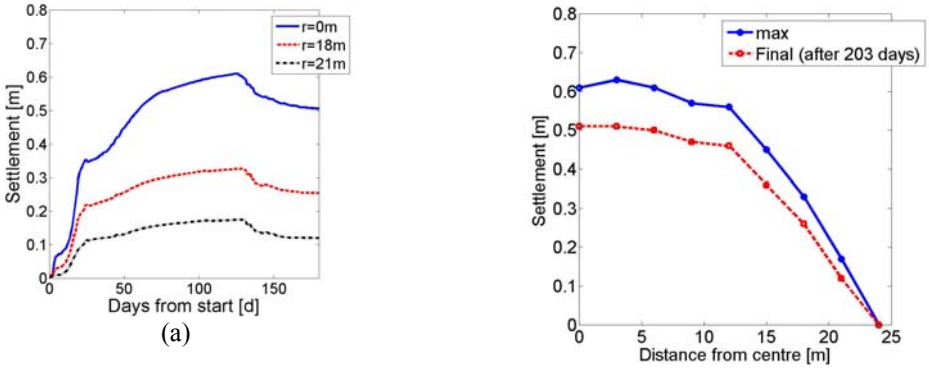

Figure 4. Porto Romano. Settlement versus time in terms of location measured by the inclinometer.

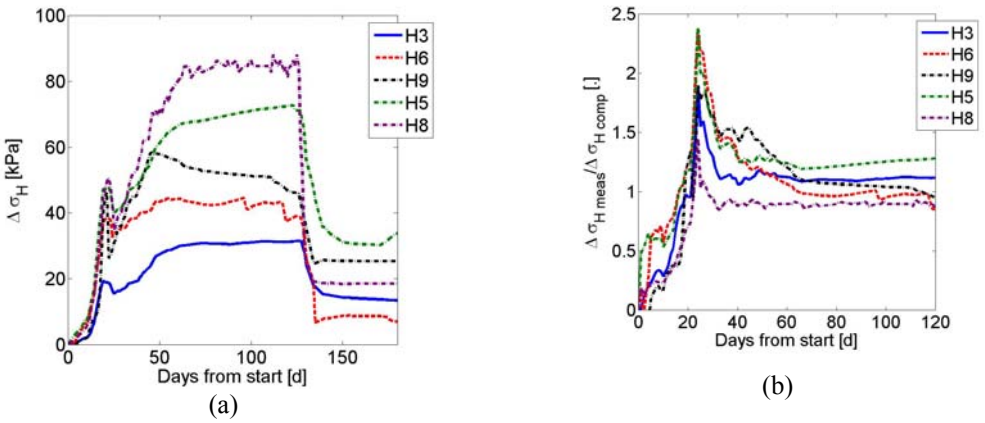

Figure 5. Porto Romano. (a) The measured effective horizontal stress normalized to have zero initial stress in terms of time and device, (b) The ratio of the measured over computed by elastic theory effective horizontal stress induced by the preload embankment in terms of time and device.

3. ANALYSIS OF THE FIELD TEST

The measured maximum and final settlements, or equivalently vertical strain, versus depth can be compared with computed settlements by the commonly-used method based on the coefficient of compressiblity measured in laboratory oedometer tests. The method involves two steps: (a) estimation of increase of vertical stress induced by the preload embankment based on elastic theory (Stamatopoulos and Kotzias, 1985) and (b) estimation of maximum and final settlements considering the increase in vertical stress, the maximum past effective stress and the virgin and unloading/ reloading coefficients of compressibility. Fig. 2b compares measured with computed vertical strain in terms of depth. It can be seen that computed strains are similar to the measured ones. During embankment construction, the effective horizontal stresses can be compared with those predicted from elastic theory (Poulos and Davis, 1974). Fig. 5b gives the ratio of the measured by computed effective horizontal stress induced by the preload embankment in terms of time and device. The unloading phase is not included, because in this case the theoretical value does not hold. It can be observed reasonable agreement between measured and predicted values, especially at the final stages of embankment construction, when we are not near failure, and thus elastic theory can be applied. After embankment demolition, the effective residual horizontal stresses (Δσh-res) can be compared with those predicted from theoretical considerations. The Mayne and Kulhaway (1982) empirical relationship is used. It predicts Ko in terms of OCR and the friction angle, φ', as:

$$Ko = (\sigma' h / \sigma' v) = (1 - \sin\varphi') \, OCR^{\sin\varphi'} \quad (1)$$

Using the typical friction angle of 30°, it is inferred that Δσh-res can be estimated as:

$$\Delta\sigma h\text{-res} = 0.53\ \sigma' g\ (OCR_a^{0.47} - OCR_b^{0.47}) \quad (2)$$

where σ'g is the effective geostatic stress prior to the application of preloading, OCR_b is the overconsolidation ratio at the site prior to the application of preloading and OCR_a is the overconsolidation ratio after the application of preloading. Table 3 compares the measured to estimated values. Reasonable agreement exists. The liquefaction cyclic strength is estimated versus depth using the state-of-the-art procedures (European Standard, 2003, European Prestandard, 1994, Idriss and Boulanger, 2006) for all field tests performed in the site: Standard Penetration Tests, Cone Penetration Tests and geophysical tests measuring the shear wave velocity, Vs. Table 3 compares the average SR_{15}, in terms of the measurement, for the two soil layers that liquefy. It can be observed that all field procedures generally produce similar results: Average pre-improvement liquefaction cyclic strength (a) from depths 3 to 7m equals 0.46-0.49 and (b) from depths 7 to 15m equals 0.40-0.54. The increase of cyclic strength induced by preloading from depths 3 to 7m equals 10 to 30% and (b) from depths 7 to 15m equals 10 to 40%. The range of the results is consistent with the non-homogeneous characteristics of soils and the different methods applied. In addition, for the measured increase of cyclic strength with preloading, based on results of laboratory tests, Stamatopoulos et al. (2012) propose the following equation:

$$SR_{15-aft} / SR_{15-bef} = OCR_{aft}^{0.04/SR_{15}} \quad (3)$$

Table 3 illustrates that the predictions of equations (3) are consistent with the measurements. Furthermore the increase in cyclic strength with preloading can be explained from the increase in horizontal stress and decrease in volume through the vertical strain. In particular the effect of horizontal stress on the cyclic soil strength has been studied in the tortional-shear device by Ishihara and Takatsu (1979). Based on this expression,

$$SR_{15\text{-aft}} / SR_{15\text{-bef}} = (1 + 2\ K_{o\text{-aft}}) / (1 + 2\ K_{o\text{-bef}}) \quad (4)$$

Based on equation (2) that was verified in the field, equation (4) predicts an increase in the cyclic strength in the layer at depth 3.7-7m at the order of 1.2 and at the layer at depth 7-15m of about 1.1. The measured vertical strain of 0.05 in both layers corresponds to change in void ratio of 0.05*(1+e), or about 0.08. Assuming that for sands (e_{max}-e_{min}) equals about 0.4, the corresponding change in relative density equals 20%. For an increase in relative density of 25%, according to Ishihara (1996) the cyclic strength increases by about 20%, as a factor of 1.2. It is inferred that combined effect of both the measured increase in density and horizontal stress using expressions proposed by Ishihara and Takatsu (1979) and Ishihara (1996) predict an increase of cyclic strength induced by preloading in the layer at depth 3.7-7m at the order of 1.4 and at the layer at depth 7-15m of about 1.3, or of the same order as that obtained from SPT/CPT/VS measurements.

Table 3. Measured and predicted increase of liquefaction cyclic strength by preloading

	Measured									Predicted by eq. (3)		Predicted by eq. (4)
	$SR_{15\text{-bef}}$			$SR_{15\text{-aft}}$			$SR_{15\text{-aft}}/SR_{15\text{-bef}}$			OCR_{aft}	$SR_{15\text{-aft}}$ / $SR_{15\text{-bef}}$	$SR_{15\text{-aft}}$ / $SR_{15\text{-bef}}$
Depth	N_{SPT}	CPT	Vs	N_{SPT}	CPT	Vs	N_{SPT}	CPT	Vs			
3.7-7m	0.44	0.46	0.38	0.46	0.49	0.49	1.1	1.1	1.3	5.0-3.2	1.2-1.1	1.4
7-15m	0.38	0.3	0.26	0.42	0.40	0.54	1.1	1.3	1.5	3.2-1.8	1.2-1.1	1.3

4. NUMERICAL SIMULATIONS

For the purpose of studying numerically the effect of soil preloading technique on the improvement of

liquefiable sandy profiles to shaking, a structure founded on a layered soil/rock model is considered. The soil profile is composed principally of 20m of loose sand (i.e. a relative density Dr < 50%) and it is divided in four layers. The shear modulus of the soil increases with depth. The average shear wave velocity $V_{s,30}$ computed only in the upper 20m of the soil profile is 213m/s. The fundamental elastic period of the soil profile is 0.38s. The ECP's elastoplastic multi-mechanism model (Aubry et al. 1982; Hujeux 1985) is used to represent the soil behaviour on the top 20m. For the bedrock, isotropic linear elastic soil behaviour is assumed with a Vs equal to 550m/s. The deformable bedrock is placed at 20m depth. The ground water table level is placed at 1m below the surface. So as to take into account the interaction effects between the structure and the plane-strain domain, a modified width plane strain condition (Saez 2008) was assumed in the finite element models. In this case a width of 4m is used.

In order to investigate the effect of the preloading method on the response of both the soil profile and the structure, a comparative dynamical response analysis at the end of shaking for the cases with and without mitigation method is done. Concerning the two-story concrete building its total height is 4.2m and the width is 4.0m. The mass of the building is assumed to be uniformly distributed along beam elements and the columns are supposed massless. The total mass of the building is 40T. With these characteristics the fundamental period of the structure (T_{str}) is equal to 0.24s. In order to simulate the structure plastic hinge beam-column elements are used. The model is based on the two-component model presented by Giberson (1969) and the modifications introduced by Prakash et al. (1993) to take into account axial force and bending moment interaction. Finally, a rigid block of 0.1x6x4m is used to simulate the foundation.

The elastoplastic multi-mechanism model developed at Ecole Centrale Paris, known as ECP model is used to represent the soil behaviour. This model can take into account the soil behaviour in a large range of deformations. The model is written in terms of effective stress. The representation of all irreversible phenomena is made by four coupled elementary plastic mechanisms: three plane-strain deviatoric plastic deformation mechanisms in three orthogonal planes and an isotropic one. The model uses a Coulomb type failure criterion and the critical state concept. The evolution of hardening is based on the plastic strain (deviatoric and volumetric strain for the deviatoric mechanisms and volumetric strain for the isotropic one). To take into account the cyclic behaviour a kinematical hardening based on the state variables at the last load reversal is used. The soil behaviour is decomposed into pseudo-elastic, hysteretic and mobilized domains. Refer to Aubry et al. (1982), Hujeux, (1985) among others for further details about the ECP model. The soil model's parameters are obtained using the methodology suggested by Lopez-Caballero et al. (2007). Fig. 6a shows the responses of the drained cyclic shear tests obtained by the model of the sand at p'_o=30, 50, 100 and 150kPa. The tests results are compared with the reference curves given by Seed et al. (1986). The obtained curves of cyclic stress ratio (SR = $\sigma_{v-cyc}/(2 \cdot p'_o)$, with σ_{v-cyc} the cyclic vertical stress applied in the cyclic loading) in a triaxial path with isotropic consolidation as a function of the number of loading cycles to produce liquefaction (N) at p'_o=30, 50 and 100kPa are given in Fig. 6b. The modelled test results are compared with the reference curves given by Seed and Idriss (1982) for sands at different densities (i.e. SPT values).

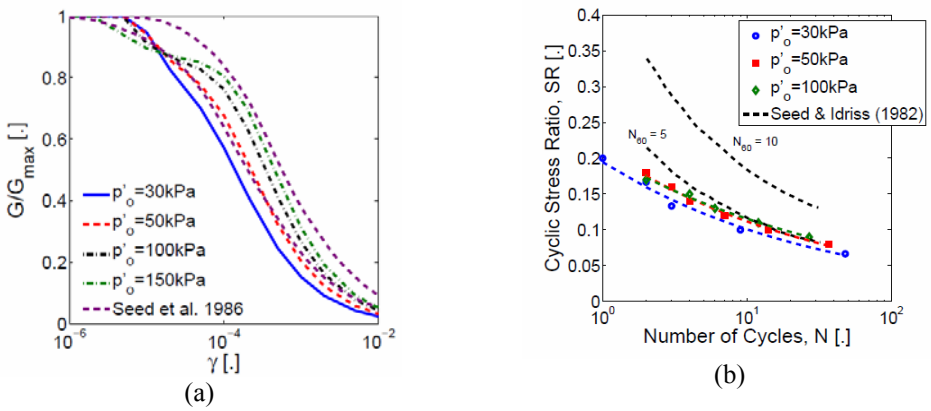

Figure 6. Simulated a) G/G_{max}-γ and b) liquefaction curves for the sand model

In order to simulate the construction and demolition of the preload embankment, the calculations are performed in two steps. In the first step, since for nonlinear elastoplastic models soil behaviour is a function of the effective stress state, initial *in-situ* stress state due to gravity loads are computed. After this initialization, the initial effective stresses, pore-water pressures and model history variables are stored to be used as initial state of the second step computation. In the second one, a sequential level-by-level construction and demolition of the embankment is performed. The embankment load is applied as a prescribed normal stress time history at the surface of soil profile. In order to assess the effect of applied load on the response of the soil profile, two embankment heights were studied, 5 and 9m with a density equal to 1900kg/m^3. The dimensions of the base and the crest of the embankment are 18 and 2m respectively. The embankment is constructed and demolished in 23 days and it stays in place during 11 days before the application of the seismic event. After this period, all over pore pressures are dissipated.

In order to define appropriate input motions to the non-linear coupled dynamical analysis, a selection of recorded accelerograms is used. The adopted earthquake signals are proposed by Iervolino and Cornell (2005) and Kayhan et al. (2011). Thus, 34 unscaled records were chosen from the Pacific Earthquake Engineering Research Center (PEER) database. The events range in magnitude between 5.2 and 7.6 and the recordings are at site-to-source distances from 15 to 50km and dense-to-firm soil conditions (i.e. 360m/s < Vs 30m < 800m/s).

5. ANALYSIS OF NUMERICAL SIMULATION RESULTS

In this section, the change in soil state due to the construction and demolition of the embankment is first analyzed. Fig. 7a displays the distribution of $\Delta\sigma_{zz}$ induced into the soil foundation at the end of the embankment construction (H_{embk}=5m). As expected, the application of preloading produces an overconsolidation on the soil (PR). As shown in Fig. 7b the embankment load influences the soil behavior down to 5m deep (i.e. PR>2). Thus, it is expected that it produces a soil stiffening effect that allows a reduction of the pore pressure excess during the earthquake. In addition, comparing the induced horizontal effective stress (σ_{yy}) along the soil depth (Figures 7c, 7e), it is interesting to note that near the surface level, a residual σ_{yy}, which is a function of the embankment height, appears at the end of the demolition of the embankment. Figures 7d and 7f display the settlement evolution obtained during the construction and demolition of the preload embankment, as well as the permanent settlement. It is noted that a permanent settlement is obtained at the end of the demolition of the embankment.

So as to show the effect of preloading on the soil response, Fig. 8 displays a comparison of the evolution of liquefaction ration ($r_u = \Delta P_w/\sigma'_{vo}$) as a function of time and depth for the same input earthquake in a case with and without preloading. It is noted that for the case where the preload was used a reduction in the r_u value is found. It is well known that a co-seismic settlement appears with the liquefaction apparition. As already mentioned, the remediation method used increases the liquefaction strength and in consequence it will decrease the soil settlement (Fig. 9a and b). As expected, the higher the embankment height, the higher the settlement reduction. It can be also seen, for example, that for H_{embk}=5m, the reduction is most important for the settlements lower than 10cm. However, despite that a settlement reduction appears, due to the soil stiffening effect, the structural deformation levels (i.e. interstory drift ISD) are increased (Fig. 9c and d). It is noted that, the higher the embankment height, the higher the ISD values. Hence, the use of a big embankment could be an unfavorable method from the structural viewpoint.

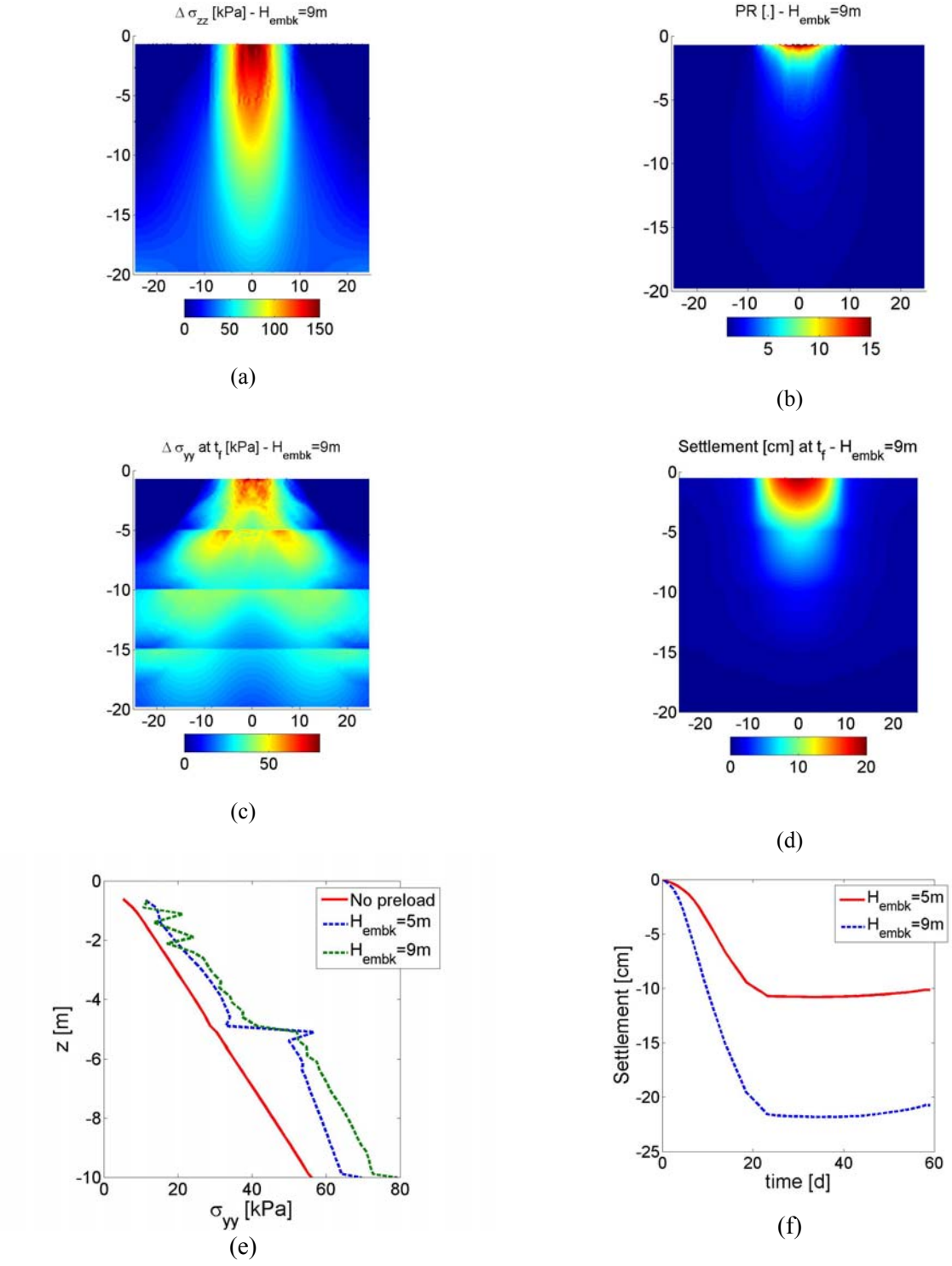

Figure 7. Effect of embankment on a) the induced $\Delta\sigma_{zz}$, b) the induced pre-stress ratio (PR), c) the induced $\Delta\sigma yy$ after the application of preloading, and d) the induced settlement). Also, e) the evolution of σ_{yy} along the soil depth under the foundation centreline and f) settlement evolution obtained during the construction and demolition of the preload embankment.

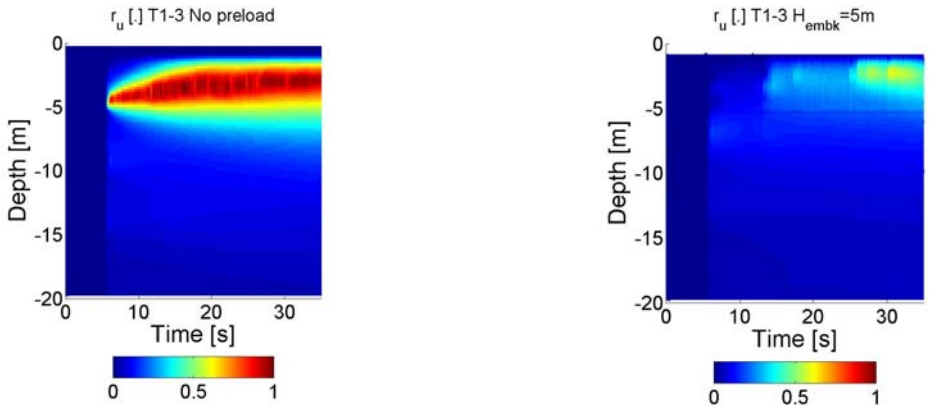

(a) (b)

Figure 8. Comparison of liquefaction ratio evolution in time and depth for a case a) without and b) with preloading.

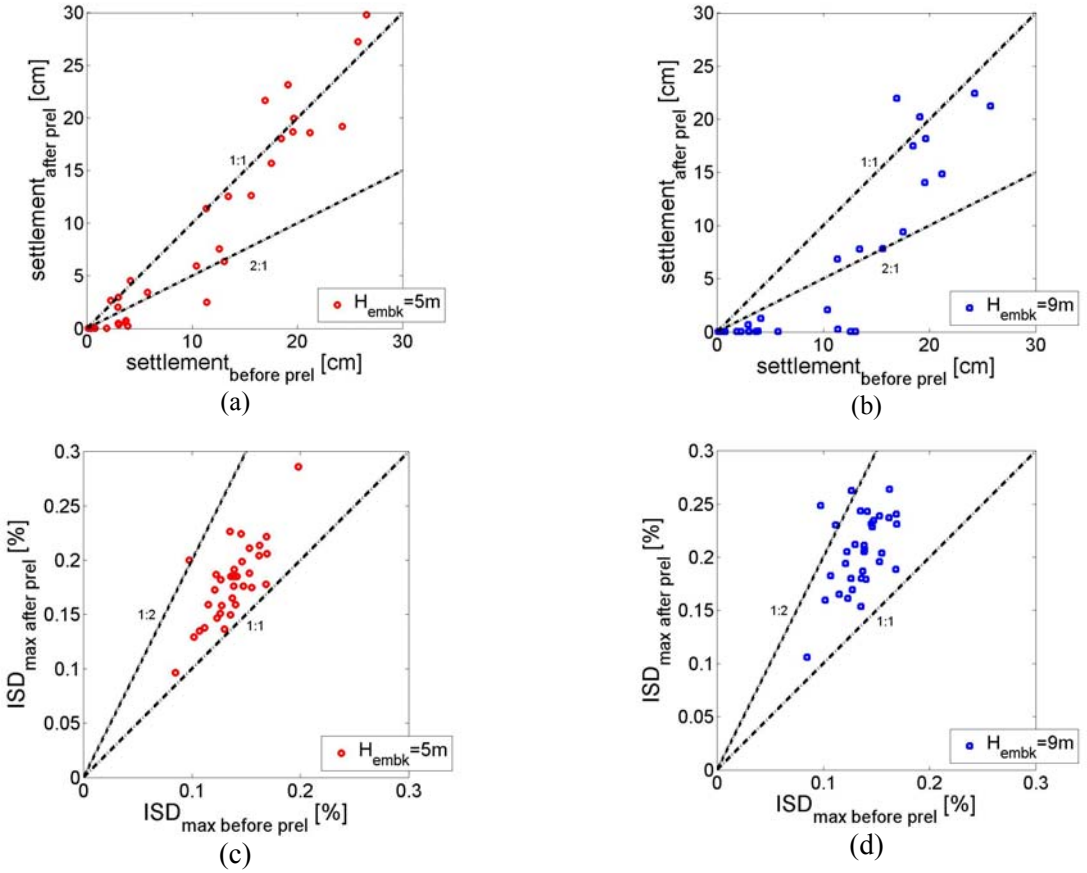

Figure 9. Effect of embankment on a) and b) the obtained co-seismic settlement values and c) and d) the obtained interstory drift of the building.

CONCLUSIONS

The use of preloading technique to improve liquefiable sites is studied. An important field test campaign on a liquefaction susceptible sandy site at Porto Romano in Albania was performed in order to measure the initial soil properties and their evolution as well as the stress state after the construction and demolition of an embankment. The measurements showed some increase in soil properties SPT,

CPT and Vs and horizontal stresses which using empirical relations predict an increase in sites cyclic strength. These results are comforted by performing numerical simulations of a similar site where the effect of construction and demolition of two embankments with different heights are studied.

The results show that the preloading has a beneficial effect when the co-seismic settlements are not important and even more for higher height of embankment. However, the seismic analysis of a two storey building on the mitigated site showed that higher damage in terms of inter storey drift should be expected for the higher embankment.

AKCNOWLEDGEMENT

The work is funded by the Seventh Framework Programme of the European Community, European Commission Research Executive Agency under grant agreement FP7-SME-2010-1-262161-PREMISERI. The borings and SPT and CPT tests were performed by Geostand Co. The geophysical investigations and constuction and demolition of the preload embankment were performed by Altea Geostudio Co of Albania.

REFERENCES

Aubry, D., Hujeux, J.-C., Lassoudière, F. and Meimon, Y. (1982). A double memory model with multiple mechanisms for cyclic soil behaviour. *Int. Symp. Num. Mod. Geomech*, pages 3–13. Balkema.

Committee on Earthquake Engineering, Commission on Engineering and Technical Systems, National Research Council (1985). Liquefaction of soils during earthquakes. National Academy Press, Washington, D. C.

European Standard (2003) Eurocode 8: Design of structures for earthquake resistance, Final Draft, prEN 1998-5, December.

European Prestandard (1994). Eurocode 8 - Design provisions of earthquake resistance of structures - Part 5: Foundations, retaining structures and geotechnical aspects.

Giberson, M. (1969). Two nonlinear beams with definitions of ductility. *Journal of Structural Division, ASCE* **95 :2**, 137–157.

Hujeux, J.-C. (1985). Une loi de comportement pour le chargement cyclique des sols. *In Génie Parasismique*, pages 278–302. V. Davidovici, Presses ENPC, France.

Idriss, I. M., and Boulanger, R. W. (2006). Semi-empirical procedures for evaluating liquefaction potential during earthquakes. *Journal of Soil Dynamics and Earthquake Engineering* **26:**, 115-130.

Iervolino I. and Cornell C.A., 2005. Record Selection for Nonlinear Seismic Analysis of Structures, *Earthquake Spectra,* Volume **21**, No. **3**, pages 685–713.

Ishihara K. (1996). Soil behaviour in Earthquake Geotechnics. Clarendon Press, Oxford, UK.

Ishihara K. and Takatsu H. (1979). Effects of overconsolidation and Ko conditions on the liquefaction characteristics of sands. *Soils and Foundations* **19:4**, 59-68.

Kayhan A.H., Korkmaz K.A., Irfanoglu A. (2011). Selecting and scaling real ground motion records using harmony search algorithm. *Soil Dynamics and Earthquake Engineering*, **31,** 941–953.

Lopez-Caballero, F., Modaressi-Farahmand-Razavi, A., and Modaressi, H. (2007). Nonlinear numerical method for earthquake site response analysis I- elastoplastic cyclic model & parameter identification strategy. *Bulletin of Earthquake Engineering*, **5:3**, 303–323.

Mayne P. W. and Kulhway F. W. (1982). Ko-OCR relationships in Soils. *Journal of the Geotechnical Engineering Division, ASCE* **108:6**, 851-872.

Poulos, H.G. and Davis, E.H. (1974). Elastic Solutions for Soil and Rock Mechanics. John Wileys, New York.

Prakash, V., Powel, G.H. and Campbell, S. (1993). DRAIN 2D-X, Base program description and User Guide.

Seed, H. B. and Idriss, I. M. (1982). Ground motion and soil liquefaction during earthquakes. Monograph series, earthquake engineering research institute, University of California, Berkeley, CA.

Seed, H. B., Wong, R. T., Idriss, I. M., and Tokimatsu, K. (1986). Moduli and damping factors for dynamic analyses of cohesionless soils. *Journal of Geotechnical Engineering - ASCE*, **112:11**, 1016–1032.

Saez, E. (2008). Dynamic non-linear Soil-Structure Interaction. PhD thesis, Ecole Centrale Paris, France.

Stamatopoulos A. C and Kotzias P. C. (1985). Soil Improvement by Preloading. John Wiley & Sons.

Stamatopoulos C., Petridis P., Bassanou M. and Stamatopoulos A. (2005). Increase in horizontal stress induced by preloading. *Ground Improvement* **9:2**, 47-51.

Stamatopoulos, C.A , Lopez-Caballero F. and Modaressi-Farahmand-Razavi A. (2012). Laboratory tests and numerical simulations giving the effect of preloading on the cyclic liquefaction strength, *15WCEE*, Lisboa, Portugal.